2780 *Macromolecules* **2010**, *43*, 2780–2788
DOI: 10.1021/ma902297b

Macromolecules
ARTICLE

# Molar Mass and Molecular Weight Distribution Determination Of UHMWPE Synthesized Using a Living Homogeneous Catalyst

**Saeid Talebi,[†] Rob Duchateau,[†] Sanjay Rastogi,*[,†,§] Joachim Kaschta,[∥] Gerrit W. M. Peters,[‡] and Piet J. Lemstra[†]**

[†]*Department of Chemical Engineering and Chemistry, and* [‡]*Department of Mechanical Engineering, Eindhoven University of Technology, P.O. Box 513, 560 0MB Eindhoven, The Netherlands,* [§]*Department of Materials, Loughborough University, Leicestershire LE11 3TU, Loughborough, England, United Kingdom, and* [∥]*Institute for Materials Science, University of Erlangen-Nürnberg, Erlangen, Germany*

*Received October 15, 2009; Revised Manuscript Received January 28, 2010*

ABSTRACT: Understanding of the physical characteristics of a polymer requires molar mass determination. For the commercially available polymers, having average molar mass below 1 000 000 g/mol, chromatography is the method that is often applied to determine the molar mass and molar mass distribution. However, the application of conventional chromatography techniques for polymers having molar mass > 1 000 000 g/mol becomes very challenging, and often the results are disputed. In this article, melt rheometry based on the "modulus model" is utilized to measure the molar mass and polydispersity of ultra high-molecular-weight polyethylenes (UHMWPEs) having molar mass > 1 000 000 g/mol. Results are compared with the chromatography data of the same polymer samples and the boundary conditions where the chromatography technique fails, whereas the rheometry provides the desired information is discussed. The rheological method is based on converting the relaxation spectrum from the time domain to the molecular weight domain and then using a regularized integral inversion to recover the molecular weight distribution curve. The method is of relevance in determining very high molar masses (exceeding 3 000 000 g/mol) that cannot be ascertained conclusively with the existing chromatography techniques. For this study, UHMWPEs with various weight-average molar masses, where the number-average molar mass exceeds > 1 000 000 g/mol, are synthesized. Catalyst used for the synthesis is a living homogeneous catalyst system: MAO-activated bis(phenoxy imine) titanium dichloride. The rheological behavior of the thus synthesized nascent reactor powders confirms the disentangled state of the polymer that tends to entangle with time in melt.

## Introduction

The polyolefin synthesis is dominated by the use of multisited heterogeneous Ziegler−Natta catalysts. However single-site catalysts are finding an exceptional role in the polymer industry.[1] The advantage of single-site catalysts over classical Z−N catalysts is their capability to produce tailormade polymers with controlled molecular weight, specific tacticity, and a narrow molecular weight distribution.[2] The ultimate control is obtained with a living catalyst because it allows us to fine-tune the molecular weight, form block copolymers, or form end-functionalized polyolefins while maintaining a very narrow polydispersity (PDI).

Group 4 metal phenoxyimine complexes, invented by scientists at Mitsui,[3] provide an interesting class of living olefin polymerization catalysts. These catalysts have been used in different laboratories, and progress in the area of stereoselective as well as living olefin polymerization has been reported.[4,5] Fujita et al. have demonstrated that when activated with MAO, the bis(phenoxyimine) titanium complex, [2-(*t*-Bu)-$C_6H_3O(CHNC_6F_5)]_2$-$TiCl_2$, is producing an ethylene polymerization catalyst that is living at room temperature. The reported highest molar mass that they obtained in 1 min of polymerization was $\sim 4.5 \times 10^5$ g/mol.[6] Carrying out the same polymerization at room temperature for 5 min, Sharma[7] reported synthesis of polyethylene with molar mass > 1 000 000 g/mol. However, because of the limited reliability of the applied GPC method, the mentioned molecular weight remained disputable. Using melt rheometry as a characterization method, in this article it will be demonstrated that the titanium complex is capable of producing ultra high-molecular-weight polyethylene (UHMWPE) with molar mass exceeding $9 \times 10^6$ g/mol, still in a controlled manner.

The use of homogeneous polymerization catalysts provides a novel route to produce disentangled polymer crystals directly in a reactor. Upon polymerization at low temperatures, the growing chains experience a "cold" environment and crystallize individually into folded-chain crystals, ultimately forming "monomolecular crystals", viz. one long chain forms one crystal. In fact, this is an easy and direct approach toward highly disentangled chains.[8,9] Upon melting, such a disentangled semicrystalline polymer provides a disentangled polymer melt, which is a thermodynamically unstable and relatively low viscous state. To achieve the thermodynamically stable melt state, chains tend to entangle with time. The presence of fewer entanglements in the initial stages of the disentangled melt lead to higher molar mass between entanglements and thus a lower elastic modulus of the melt. Figure 1 shows a typical time sweep experiment performed on two different disentangled polyethylenes having average molar masses of (2.0 and 5.3) $\times 10^6$ g/mol, respectively. From here it is evident that the time required for the modulus build-up increases with the increasing molar mass. Ultimately, the initially disentangled chains entangle to form the thermodynamically stable melt state. Stress relaxation and frequency sweep measurements are performed on the fully entangled samples. Because of

*Corresponding author. E-mail: s.rastogi@lboro.ac.uk.

 Published on Web 02/23/2010 

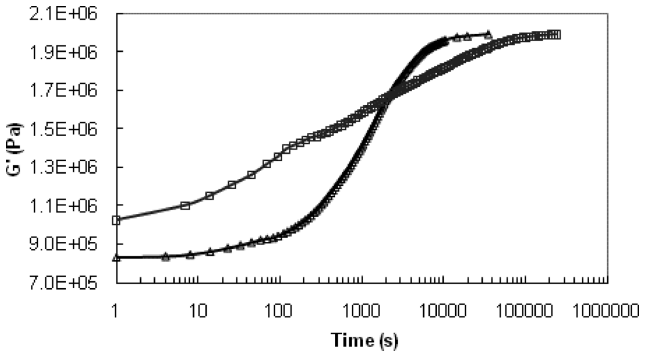


**Figure 1.** Modulus build up in an initially disentangled polymer having molar mass of $2.0 \times 10^6$ (△) and $5.3 \times 10^6$ (□) g/mol as a function of time. Experiments are performed at a constant temperature 160 °C, fixed frequency 10 rad/s, and a strain of 1%, respectively. The absolute values of elastic modulus at $t = 0$ are questionable because of the uncertainties associated with the time required for reaching the thermal stability. The time $t = 0$ refers to the time when the polymer has reached the thermal stability.

**Scheme 1. Schematic Structure of the Bis(phenoxyimine) Titanium Catalyst Precursor, [2-(*t*-Bu)-$C_6H_3O(CHNC_6F_5)]_2TiCl_2$**

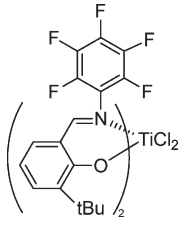


the high melt viscosity of the molar mass used, the stress-relaxation experiments have advantage over the creep measurements.

## Experimental Section

**Materials.** All manipulations are performed under an argon atmosphere using a glovebox (Braun MB 150 GI) and Schlenk techniques. Solvents are purchased from VWR. Dry solvents are prepared by passing them over a column containing $Al_2O_3$ and degassed at least twice prior to use. The bis(phenoxyimine) titanium complex, [2-(*t*-Bu)-$C_6H_3O(CHNC_6F_5)]_2TiCl_2$ (Scheme 1) and methyl aluminoxane (MAO) are used as received from MCAT GmbH and Aldrich, respectively. Ethylene (4.5 grade supplied by Air Liquid) is purified by passing over columns of BTS copper catalyst and 0.4 nm molecular sieves.

**Polymerization.** Polymerizations have been performed under an inert atmosphere by using a glass reactor (1 L) equipped with a mechanical stirrer and a temperature probe. Solvent is introduced to the nitrogen-purged reactor and is thermostatted to the prescribed polymerization temperature and saturated with ethylene (1 bar pressure). MAO is added prior to the precatalyst to scavenge residual impurities. The polymerization is initiated by the addition of the precatalyst. After a set time, the polymerization is terminated by the addition of acidified isopropanol. The resulting polyethylene is collected by filtration, washed with acetone and water, then dried under vacuum at 60 °C overnight.

**Rheometry.** Oscillatory shear measurements and stress relaxation in the linear viscoelastic (LVE) regime are performed using a Rheometrics rms 800 strain controlled spectrometer at 160 °C, angular frequencies (0.001 to 100 rad/s) and strains 0.5%. By performing strain sweeps, the LVE region is established. Because of the high sample stiffness, parallel plate geometry is used with a disk diameter of 8 mm. Sample thickness is 1 mm. For the high-molar-mass materials, stress relaxation experiments are performed to expand the time window of the measurements. All experiments in this article are performed on fully entangled samples. Prior to the measurements, the disentangled nascent powders are first sintered at 50 °C and 200 bar, and the thus obtained disks of 8 mm diameter from the sintered powder are heated fast (~30 °C/min) to well above the equilibrium melting temperature in the rheometer. Time sweep experiments, at a fixed frequency and strain, were performed on the initially disentangled samples until no change in elastic modulus was observed. No change in the elastic modulus is indicative of the fully entangled state. Stress relaxation and frequency sweep experiments are performed on the fully entangled polymers by applying strain amplitude in the linear viscoelastic regime.

Possible slippage between the sample and rheometer discs is checked with the help of an oscilloscope. During dynamic experiments, two output signals from the rheometer, that is, one signal corresponding to sinusoidal strain and the other to the resulting stress response, are monitored continuously by an oscilloscope. A perfect sinusoidal stress response, which can be achieved at low values of strain, shows that there is no slippage between the sample and the discs.

For all samples, 0.5 wt % Irganox 1010 is added, and measurements are performed under a nitrogen atmosphere to prevent thermo-oxidative degradation. To verify that no degradation had occurred during experiments, frequency sweep measurements performed at the beginning and the end of the experiments are compared. FTIR studies on the samples retrieved after the experiments are performed to override any possibility of cross-linking. To confirm further that the sample is dissolved in decalin, it is to be realized that the cross-linked sample will be prone to swelling rather than dissolution.

All experiments are performed at 160 °C. Because of very low glass-transition temperature of polyethylene (below −120 °C), no considerable shift could be obtained in the temperature window of 160−190 °C, and thus time−temperature superposition studies are not pursued.

**GPC.** These measurements are carried out in the group of Prof. Münstedt at the Institute of Polymer Materials, Erlangen University. A high-temperature GPC (150 °C, Waters) coupled to a high-temperature multiangle light scattering apparatus (MALLS, Dawn EOS, Wyatt Technologies) is used for the measurements. The measuring temperature is 140 °C, and 1,2,4-trichlorobenzene is used as a solvent. The flow rate is chosen to be 0.5 mL/min, and 325:l of the polymer solution is injected onto the column system consisting of three columns: Shodex UT806 M (Showa Denko, exclusion limit in polystyrene molar mass $5 \times 10^7$ g/mol) and one high molar mass separation column Shodex UT807 (exclusion limit $2 \times 10^8$ g/mol). The concentration of the polymer eluted from the columns is measured by means of two concentration detectors using different detection techniques (infrared absorption, polyCHAR IR4, and an internal differential refractive index detector).

The evaluation of the measurements is performed using ASTRA 4.73 analysis software (Wyatt Technologies). The concentration signal from the IR detector is used in the evaluation of the data because of its higher sensitivity. The determination of the absolute molar mass and of the radius of gyration, $< r_g^2 >^{0.5}$, for each eluted fraction is done in a linear Zimm plot.[10] In parallel, the same concentration signal is evaluated via the calibration curve connecting elution volume with the molar mass of polymer standards using the WinGPC 6.20 software (Polymer Standard Services). The GPC is calibrated with polystyrenes of narrow molar mass distribution characterized by $M_w/M_n$ values < 1.1. The calibration curve spans a molar mass range from 580 to 11 300 000 g/mol. For the measurements of polyethylene samples, the polystyrene calibration is converted into a polyethylene calibration using the universal calibration technique. The following Mark−Houwink parameters of $K = 0.0196$ and $a = 0.73$ (units for $K$ chosen in such a way that $M$ is grams per mole for the Staudinger index in cubic centimeters per gram) are used to correct for the different hydrodynamic

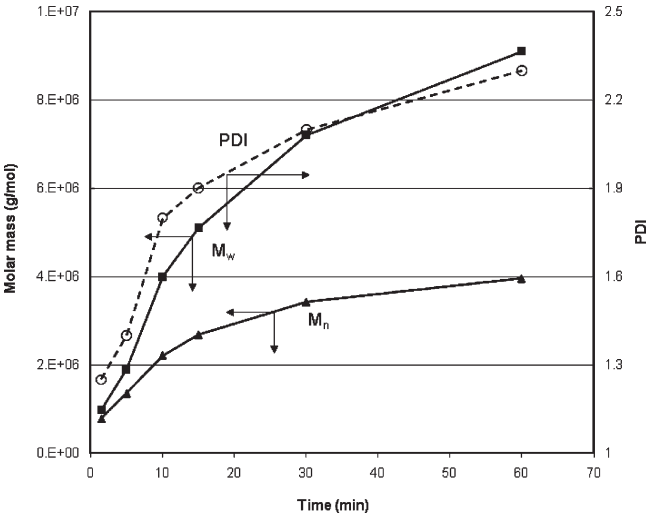


**Figure 2.** Effect of polymerization time on the $M_w$, $M_n$, and polydispersity (PDI) of UHMWPE (other polymerization parameters are constant: $T_p$ = 20 °C, 1 $\mu$mol of Ti, Al/Ti molar ratio = 8500, 1 bar of ethylene, 750 mL of toluene). The values shown here are obtained by rheological studies as described later.

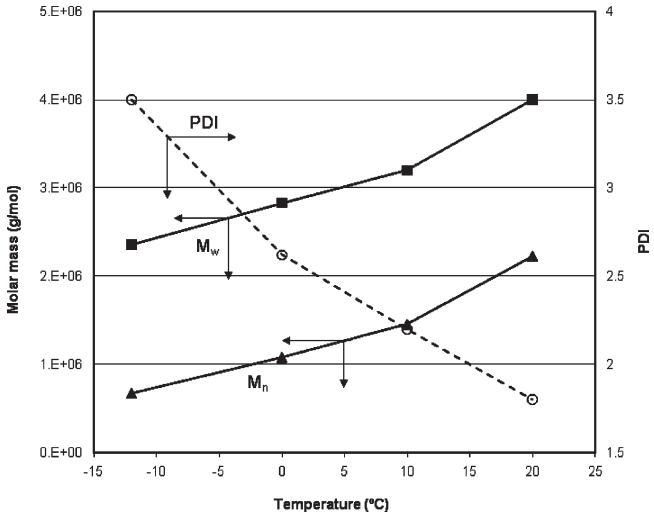


**Figure 3.** Effect of the polymerization temperature on the $M_w$, $M_n$ and polydispersity (PDI) of UHMWPE. (Other polymerization parameters are kept constant: polymerization time = 10 min, 1 $\mu$mol of Ti, Al:Ti molar ratio 8500, 1 bar of ethylene, 750 mL of toluene).

volumes of polystyrene and polypropylene in solution. All chromatograms are corrected with respect to the elution volume of the internal standard.[11]

## Results

Studies reported in this section highlight the chemistry applied for the synthesis of UHMWPE, followed by their molecular characterization, which are weight- and number-average molar mass distribution.

**Ethylene Polymerization in a Homogeneous System.** In this part, the influence of physical parameters on molecular weight and PDI of the synthesized polymer will be addressed.

*a. Polymerization Time*. Figure 2 shows the molar mass development with increasing polymerization time based on melt rheology and GPC specially calibrated for high molar masses. Melt rheology applied for determination of the molar mass will be discussed in the later stage of this paper. For short reaction times, a linear dependence between the polymerization time and the molar mass is observed that is indicative for living behavior of the catalyst. However, the PDI increases considerably with polymerization time, which indicates that the system starts to deviate from purely living. Probably, heterogenization of the catalyst and mass transport limitation within the growing polymer particles enclosing the active sites are responsible for this broadening of the PDI. The trend in Figure 2 is similar to the published data by Ivanchev et al.,[12] who suggested a gradual deactivation of the catalyst by the growing polymer after a certain polymerization time. It is to be realized that although with the polymerization time PDI increases, but for the chosen polymerization condition, the number-average molar mass exceeds 1 000 000 g/mol. Therefore, compared with the commercially available polymers, the synthesized polymers in our laboratory are not only disentangled but also possess relatively narrow molar mass distribution.

*b. Temperature*. Polymerization temperature ($T_p$) is one of the most complicated operational factors for polymerization. The solubility of ethylene in the solvent decreases with increasing temperature and, consequently, the monomer concentration drops at higher temperatures, causing a decrease in the propagation reaction.[13] Raising the temperature increases both the propagation rate as well as the probability of chain transfer reactions. Normally, chain transfer reactions have higher activation energies than insertion reactions, and a change in $T_p$ strongly affects the rate of chain termination and hence the molecular weight and PDI.[14−16] Consequently, catalysts that show living behavior at low temperature might show chain termination at elevated temperature. For example, Fujita et al. reported an optimum polymerization temperature to obtain the highest molar mass.[17]

In Figure 3, the effect of the polymerization temperature on the $M_w$ and the PDI of the obtained polymer is illustrated. The average molecular weight increases with the polymerization temperature, illustrating that raising the temperature from −15 to 20 °C does not lead to termination processes. Surprisingly, at temperatures exceeding 30 °C, at atmospheric pressure, a considerable decrease in the polymer yield is observed, suggesting thermal decomposition of the catalyst.

*c. Cocatalyst−Catalyst Ratio*. MAO is the most widely used cocatalyst in homogeneous polymerization.[18−20] The disadvantage of MAO is that it often has to be applied in large excess. This large excess of MAO also influences the polarity of polymerization medium, which might have an effect on the polymerization rate. For example, Sharma[7] found that the polymer yield continues to increase with increasing amount of MAO, even up to a staggering Al/Ti ratio of 130 000, which is difficult to explain by effects other than polarity.

The effect of the aluminum (Al)/transition metal (TM) ratio on the productivity and molecular weight for the metallocene-catalyzed polymerization of ethylene has been explored by Chein and Wang.[21] The authors have shown that a rise in Al/TM results in a decrease in the productivity and molecular weight. However, the effect of the Al/TM ratio on the molar mass of the polymer produced is still ambiguous, and different data have been reported.[22] Decrease in molar mass upon increasing the Al/TM ratio can be explained by chain transfer to aluminum due to the increasing concentration of trimethyl aluminum invariably present in MAO. In the case of the bis(phenoxyimine) titanium catalyst applied in this study, increasing the amount of MAO results in an increase rather than a decrease in molar mass (Figure 4). Chain transfer to aluminum does not seem to play a major

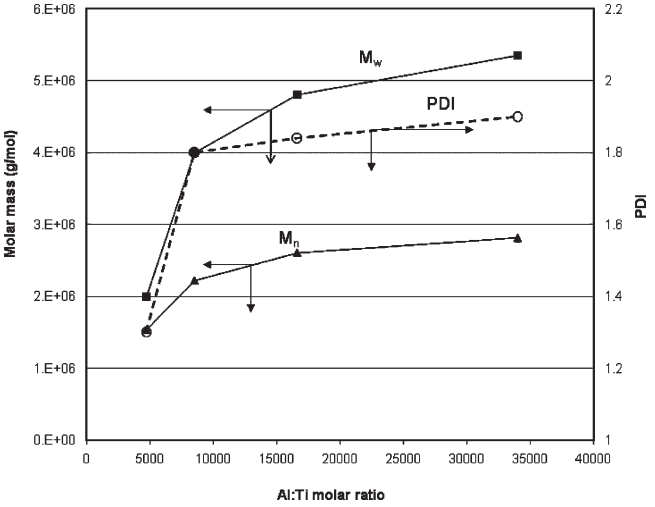


**Figure 4.** Effect of MAO/catalyst ratio on the $M_w$, $M_n$, and polydispersity (PDI) of UHMWPE (other polymerization parameters are kept constant: $T_p$ = 20 °C, polymerization time = 10 min, 1 bar of ethylene, 750 mL of toluene).

**Table 1. Molecular Weight Obtained from GPC**

| | from GPC | |
|---|---|---|
| sample batch no. | $M_w$ (g/mol)[a] | PDI |
| 1 | $2.3 \times 10^6$ | 1.9 |
| 2 | | |
| 3 | | |
| 4 | $4.3 \times 10^6$ | 2.3 |
| 5 | $5.7 \times 10^6$ | 2.1 |
| 6 | $2.4 \times 10^6$ | 1.3 |

[a] From universal calibration.

role in this catalyst system. Assuming that the catalyst is intrinsically living, the observed increase in yield and molar mass with increasing Al/Ti ratio can best be explained by the increase in the polarity of the medium with increasing MAO concentration, affording a better ion-pair separation and hence a higher polymerization rate. The increase in the PDI is assumed to be the result of heterogenization of the system.

The observed linear increase in molar mass with the polymerization time is suggestive of the living nature of the single-site catalyst used for our studies. This observation is in agreement with Fujita et al. (See ref 2.) Chain branching in these polymers is investigated following the solid-state NMR method of Pollard et al.[23] The studies performed in the melt state of the disentangled polyethylenes show the nonexistence of branches even up to the 10 000 C atoms, with the upper limit of the method applied. Therefore, it could be stated that the method used for polymerization in this publication yields linear polyethylenes that are free of branches. To determine the molar mass of the UHMWPEs, melt rheometry is applied, and the results obtained from rheometry are compared with those of the chromatography.

The samples used for rheological studies are described as sample batches 1−6. Molar masses as estimated by GPC are depicted in the Table 1. Rheological studies described in the following section show deviation in the determined molar mass and molar mass distribution by GPC of samples 4 and 5. A comparison of the GPC and rheological data is provided in Table 2. For plotting of Figures 1−4, molecular characteristics determined from rheological studies have been used.

**Determination of Molar Mass by Means of Melt Rheometry.** The molar mass and molecular weight distribution (MWD or PDI) play an important role in the processing

**Table 2. Comparison of Molecular Weight Obtained from GPC and Melt Rheometry**

| | from GPC | | from melt rheometry | |
|---|---|---|---|---|
| sample batch no. | $M_w$ (g/mol)[a] | PDI | $M_w$ (g/mol) | PDI |
| 1 | $2.3 \times 10^6$ | 1.9 | $2.0 \times 10^6$ | 1.4 |
| 2 | | | $2.8 \times 10^6$ | 2.6 |
| 3 | | | $3.8 \times 10^6$ | 2.3 |
| 4 | $4.3 \times 10^6$ | 2.3 | $5.3 \times 10^6$ | 1.9 |
| 5 | $5.7 \times 10^6$ | 2.1 | $9.1 \times 10^6$ | 2.3 |
| 6 | $2.4 \times 10^6$ | 1.3 | $1.9 \times 10^6$ | 1.3 |

[a] From universal calibration.

characteristics of the polymer, which will ultimately influence the physical and mechanical properties of the material. For instance, in melt spinning, a low-molecular-weight polymer with a broad PDI is required, whereas to produce fibers by solution spinning, a very high-molecular-weight polymer with narrow PDI is preferred. Moreover, a fundamental understanding of chain dynamics also requires the molecular characteristics of the polymer. Therefore, it is important to determine the molar mass and molar mass distribution.

Many attempts have been devoted to the estimation of rheological properties of polymer melts utilizing molecular weight and PDI data for a given polymer. However, molecular weight characterization from the rheological data, an inverse problem, has been given less attention because of its complexity that arises as a result of different views in literature, a topic beyond the scope of this article.

There are two typical models to determine the MWD from the polymer melt rheology: the "viscosity model" and the "modulus model". The viscosity model is based on the work of Bersted[24] and Bersted and Slee,[25] in which the molecular weight is related to the observed behavior in the shear rate dependent viscosity. This model has been developed by Colby, Fetters, and Graessley,[26] Malkin and Teishev,[27] Tuminello,[28] and Nichetti and Manas-Zloczower.[29] Zero shear viscosity is related to weight-average molecular weight according to

$$\eta_0 = K_1(\bar{M}_w)^{3.4} \quad (1)$$

In this article, the "modulus model" will be emphasized. According to the literature,[30] this model reflects viscoelastic properties of a polymer that correspond to the high-molecular-weight component. This model can be presented in terms of relaxation modulus, $G(t)$. This method works by converting the relaxation spectrum from the time domain to the molecular weight domain, then using a regularized integral inversion to recover the MWD curve, eq 2

$$\frac{G(t)}{G_N^0} = \left( \int_{\ln(M_e)}^{\infty} F^{1/\beta}(t, M) w(M) d(\ln M) \right)^{\beta} \quad (2)$$

$G(t)$ is normalized by the plateau modulus, $G_N^0$, $F(t,M)$ is a kernel function describing the relaxation behavior of a monodisperse component of molecular weight, $M$, where $w(M)$ is the weight fraction of the MWD function. The exponent, $\beta$, is a parameter that corresponds to the mixing behavior of the chains. For example, $\beta$ is 1 for simple reptation and 2 for the double reptation theory. $M_e$ is the average molecular weight between entanglements. The exponent $\beta$ has a significant effect on the molar mass determination. Indeed, $\beta$ indicates the nature of the polymer dynamics. Wu[31] made the molecular weight distribution calculations based on the classical (simple or single) reptation model, proposed by de Gennes,[32] that suggests $\beta = 1$.

Besides the pure reptation, another relaxation mode has been proposed by Doi and Edwards[33] named "constraint release" or "double reptation" by Rubinstein and Colby,[34] des Cloizeaux,[35] and Tsenoglou.[36] The double reptation theory imposes the exponent $\beta$ to a value of 2. A higher $\beta$ value slightly $>2$ has also been proposed in the literature,[37−40] representing the contribution of higher-order entanglements or due to the tube dilation.

One of the most successful algorithms in predicting molar mass distribution of nearly monodisperse, broad, and bimodal polymer melts is developed by Mead.[41] His calculations are based on the double reptation model, $\beta = 2$, and the single exponential kernel function.

Mead's algorithm, incorporated in the Orchestrator software[42] by Rheometrics Scientific, is used in this article. Frequency sweep experiments provide the elastic ($G'$) and loss ($G''$) moduli, the base input for the molar mass evaluation. As stated by Carrot and Guillet,[43] the accuracy of the weight-average molecular weight prediction is mainly determined by the low frequency limit of the measurements, which in this case is $10^{-3}$ rad/s. Figure 5 shows series of frequency sweep experiments performed on samples with different molar masses. Samples having lower molar masses (as anticipated by decreasing polymerization time and confirmed by GPC), batch nos. 1 and 2, show a crossover point in the range of accessible frequency of instrument, above $10^{-3}$ rad/s, but for higher molar masses, batch nos. 3 and 4, this point is shifted to lower frequency and does not occur in the measurable frequency range. Furthermore, Figure 6 shows that the elastic modulus of sample batch nos. 3 and 4 does not fall off, and the dynamic viscosity does not level off, which is a strong indication of having very high molar masses.

To extend the range of low frequencies, stress relaxation experiments are performed on the fully entangled sample. The data is converted from the time scale domain to the frequency domain. In this way, we are able to extend the low frequency data with two decades, up to $10^{-5}$ rad/s. Detailed studies on such conversion are provided in the literature,[44−46] especially by Ferry.[29] Figure 7 shows the relaxation modulus versus time for samples having different molar masses. The relaxation profile and the area under the relaxation modulus ($\eta_0 = \int G(t)\,dt$) for different samples are distinct. For each sample, the characteristic relaxation time can be obtained from the corresponding relaxation spectrum, although it is known that in the case of higher molar mass data, uncertainty in determination of the relaxation time exists.

Figure 8 illustrates the combined dynamic data for batch no. 5 covering a very large frequency range. The data in the range of $10^{-5}$ to 100 rad/s are collected from the frequency sweep experiment, and the data in the range of $8 \times 10^{-5}$ to 1 rad/s are obtained by converting relaxation data to dynamic data. The two sets of data show a good overlap. Following this method, it is possible to obtain dynamic data over almost seven decades. These data are sufficient to calculate the molar masses, but in the next part, an additional approach, time-molar mass superposition, allowing to extend dynamic data to even lower frequency such is $10^{-7}$ rad/s, will be addressed.

Recall that the molar mass determination is based on eq 2, which assumes a single exponential as the kernel function and double reptation as the framework of chain dynamics. The molar mass data obtained from the melt rheometry and GPC are summarized in Table 2. The data that are provided include weight- and number-average molecular weights, where the $M_w$ is obtained by two different techniques: light scattering and the conventional calibration method. These data and the reproducibility of the GPC runs are given in the Supporting Information because the determination of these

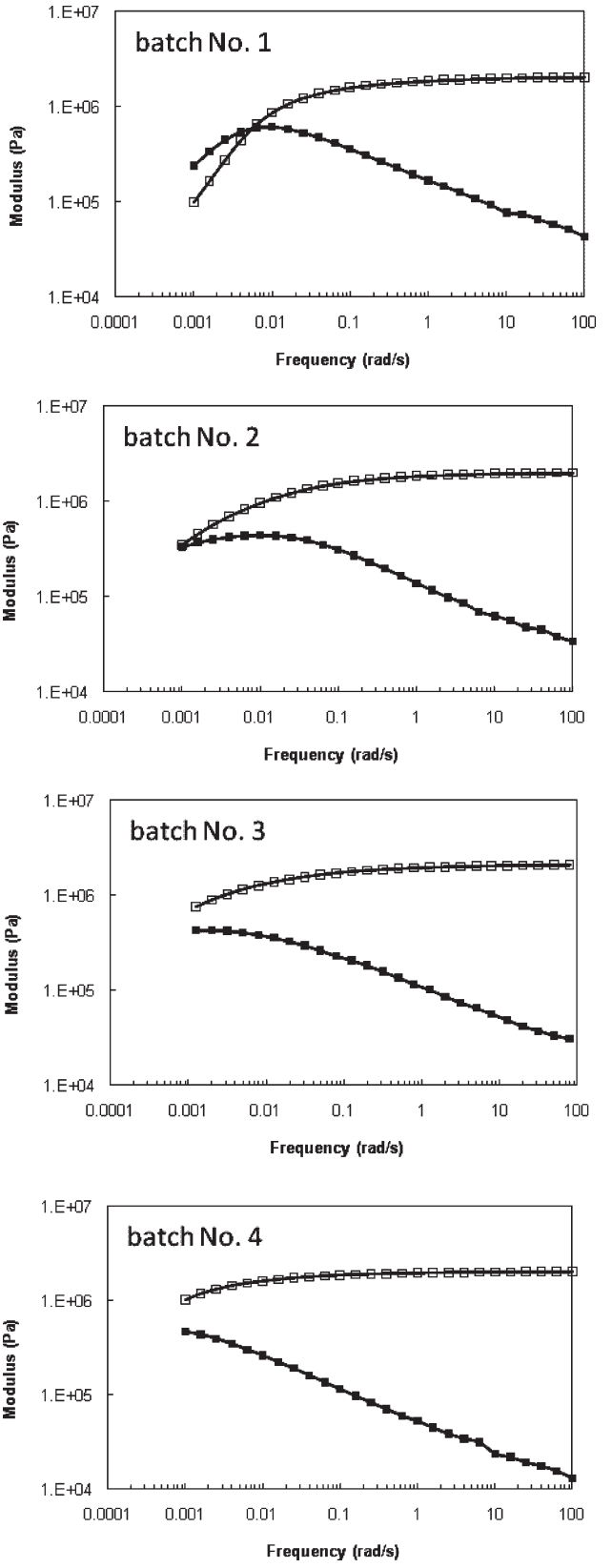


**Figure 5.** Series of frequency sweep experiments on different molar masses of UHMWPE: $G'$ (□) and $G''$ (■). The crossover point shifts to lower frequency from batch no. 1 to batch no. 2. In the case of batch nos. 3 and 4, the crossover point is not observed in the measurable frequency region.

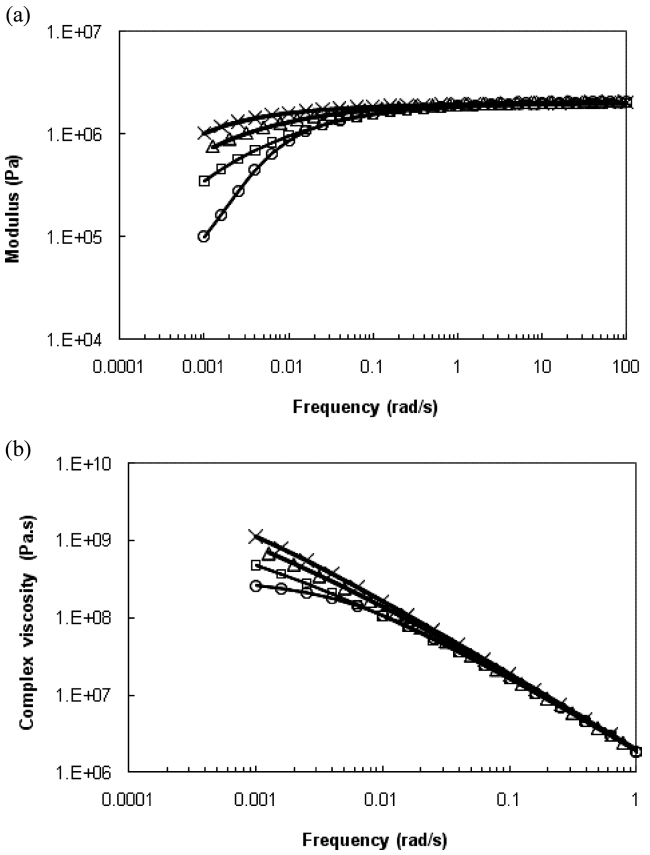


**Figure 6.** Comparison of (a) the elastic modulus and (b) the complex viscosity for different molar masses UHMWPE, batches no. 1 (○), no. 2 (□), no. 3 (△), and no. 4 (×). From batches nos. 1−4, in (a) the onset of terminal zone shifts to lower frequency, and in (b) with increasing batch number the complex viscosity shows higher values at lower frequency.

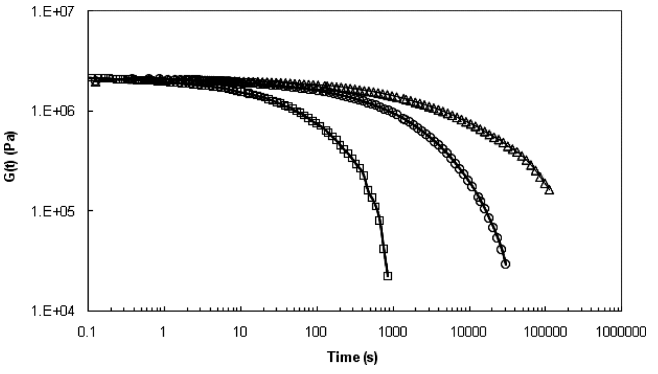


**Figure 7.** Relaxation profiles for three different batches. The data reported here is reproducible for different samples of the same batch. At least three fresh samples for each batch were investigated. The relaxation curves for batch nos. 1 (□), 4 (○), and 5 (△) clearly show the difference in molar mass. The full relaxation curve of batch no. 5 could not be obtained because of the extreme long relaxation time.

high molar masses is in itself a state of art and is beyond the scope of this publication. However, from Table 2, it is apparent that the discrepancy between the GPC and the melt rheometry data increases with the increasing molar mass. What follows is a brief summary of results obtained from GPC that highlights cause of the discrepancy.

In the case of the two batches, nos. 1 and 6, the molar masses from GPC and rheometry are within experimental limits. From Figure 7, it is clear that the relaxation modulus for batch no. 5 falls off only one decade within $10^5$ s.

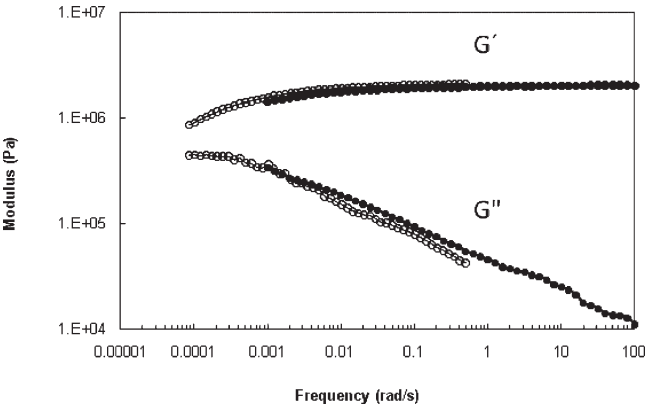


**Figure 8.** Dynamic data obtained from frequency sweep, (closed circles) and stress relaxation experiments, (open circles) for batch No. 5. Both experiments are performed at 160 °C.

**Table 3. Percentage of Mass Recovery, *r*, for Different Molar Masses (Obtained from Rheology) for the Two Different Experiments: Inject 1 and Inject 2**

| sample batch no. ($M_w$ from melt rheometry) | inject 1(%) | inject 2 (%) |
|---|---|---|
| 1 ($2.0 \times 10^6$ g/mol) | 95.7 | 92.7 |
| 4 ($5.3 \times 10^6$ g/mol) | 89.2 | 92.4 |
| 5 ($9.1 \times 10^6$ g/mol) | 85.0 | 86.7 |
| 6 ($1.9 \times 10^6$ g/mol) | 96.8 | 91.4 |

Therefore, an extremely high molar mass is expected for this sample. From melt rheometry, the calculated molar mass for this sample is $\sim 9 \times 10^6$ g/mol, whereas GPC estimates it on the order of $6 \times 10^6$ g/mol. The discrepancy between results obtained from GPC and rheology might be explained by the mass recovery from the GPC columns, *r*, of the injected polymer. The mass recovery is the ratio of detected mass obtained by the integration of the concentration signal and injected mass, $r = m_{\text{detected}}/m_{\text{injected}} \times 100\%$.

Comparing the detected mass, $m_{\text{detected}}$, with the injected mass, $m_{\text{injected}}$, it can be concluded how large the amount is of gel/insoluble material or if material is being absorbed on the columns. Table 3 summarizes the percentage of mass recovery for the measurements of the different polymers. The obtained molar mass from both GPC and rheology methods for samples having a molar mass of $\sim 2 \times 10^6$ g/mol is in very good agreement. The *r* value for those samples, batch nos. 1 and 6, is ∼95%, indicating that nearly all material is eluted from the columns and that no gel was present. The difference between the measured molar mass from the two methods for batch no. 4, having a molar mass of $5.3 \times 10^6$ g/mol (from rheology), is ∼20%, and the *r* value is ∼90%. For the sample with highest molar mass, $9.1 \times 10^6$ g/mol, *r* is $< 90\%$, and this might be the explanation for the observed discrepancy between data obtained from GPC and rheometry. Considering the decrease in mass recovery for the sample batch nos. 4 and 6, it could be stated that the chromatography method applied has limitations for determination of the ultra high molar masses.

Figure 9a−d shows GPC chromatograms and molecular weight distributions obtained from rheometry for batches 1, 4, 5, and 6. The radius of gyration is also plotted. Within the region where molar mass and molar mass distribution have been determined, the light scattering data shows linear variation in the radius of gyration with molar mass; however, in the lower molar mass region, a deviation is observed. This deviation in the molar mass indicates the existence of a molar mass component that has a higher radius of gyration than the expected value.

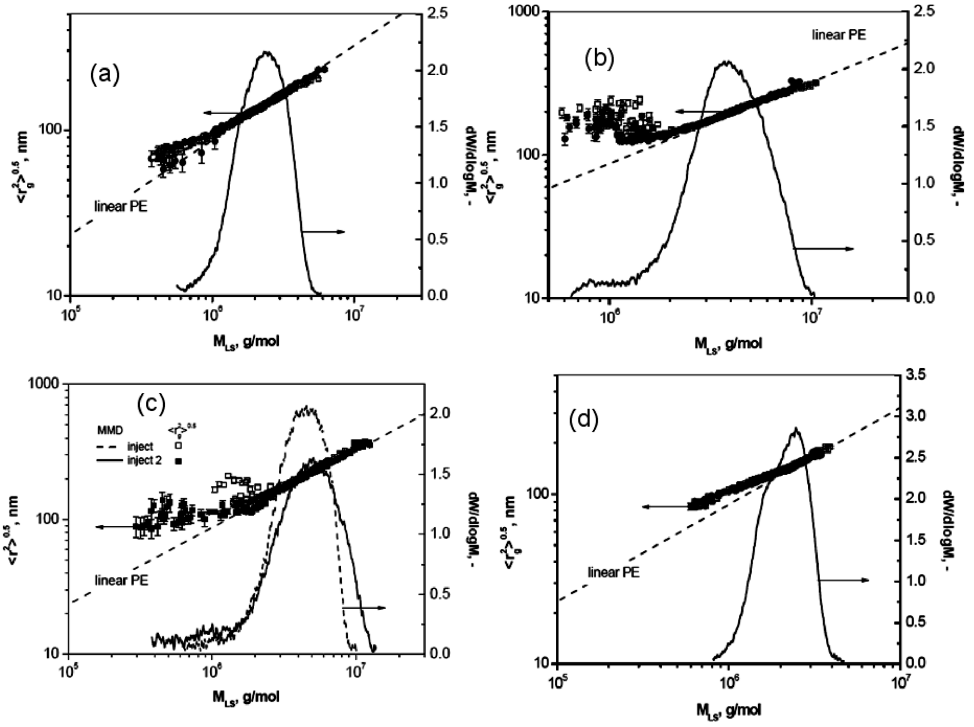


**Figure 9.** Comparing (a−d) chromatograms for batch nos. 1, 4, 5, and 6, respectively.

Detailed studies on deviation of the radius of gyration with increasing molar mass have been performed for branched polymers.[47,48] The authors have conclusively demonstrated that with an increasing branch content, the radius of gyration falls below the anticipated value for the linear polymer. Contrary to this, polymer synthesized in our laboratory shows an increase in the radius of gyration in the lower molar mass region, and thus the possible explanation of branching could be further excluded. Although, in this stage, there is no proper explanation for the deviation, from a physical viewpoint this, may be related to the difference in the chain swelling process of the disentangled state of the synthesized polymerm which may cause an increase in the radius of gyration. This calls for further experimental studies that will be pursued in the near future.

**Master Curve for Molar Mass Determination from Time-Molecular Weight Superposition.** To check the molar mass determined from the melt rheometry, an alternative approach to the dynamic behavior of UHMWPE is applied. The alternative approach combines dynamic data obtained for different molar masses. A master curve is created by shifting dynamic data to the curve for the highest molecular weight. The dynamic data for the low-molar-mass polyethylenes is retrieved from the experiments previously performed in our group.[9] Molecular characteristics of these polymers synthesized by a yttrium catalyst, having a sharp molar mass distribution within a tolerance of 1.11, are unique. Figure 10 shows the elastic and loss moduli of linear polyethylenes having molar masses $< 2 \times 10^6$ g/mol. It is evident that $G'$ and $G''$ show a similar trend for different molar masses of polyethylenes, except that they are shifted to lower frequency with increasing molar mass, demonstrating that the dynamic behavior of polymer chains with different molar mass is governed by similar underlying physics. Similar to the time−temperature superposition where one converts the temperature domain to the time domain, the molecular weight is converted to the time domain. A shift factor can be found empirically for polymers having different molar masses but similar polydispersities. Therefore, dynamic characteristics such as the crossover point and the zero shear viscosity of

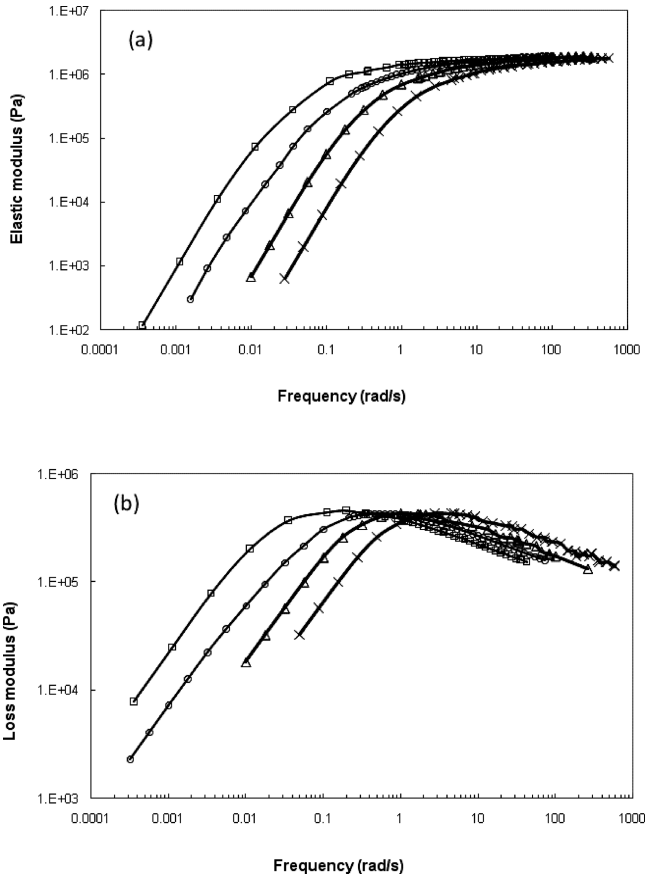


**Figure 10.** (a) Storage modulus, $G'$, and (b) loss modulus, $G''$, data for the narrow molecular weight polyethylenes (PDI ≈ 1.2) adopted from ref 9. Symbols ×, △, ○, and □ represent samples having molar mass of 430 000, 644 000, 854 000, and 1 269 000 g/mol, respectively.

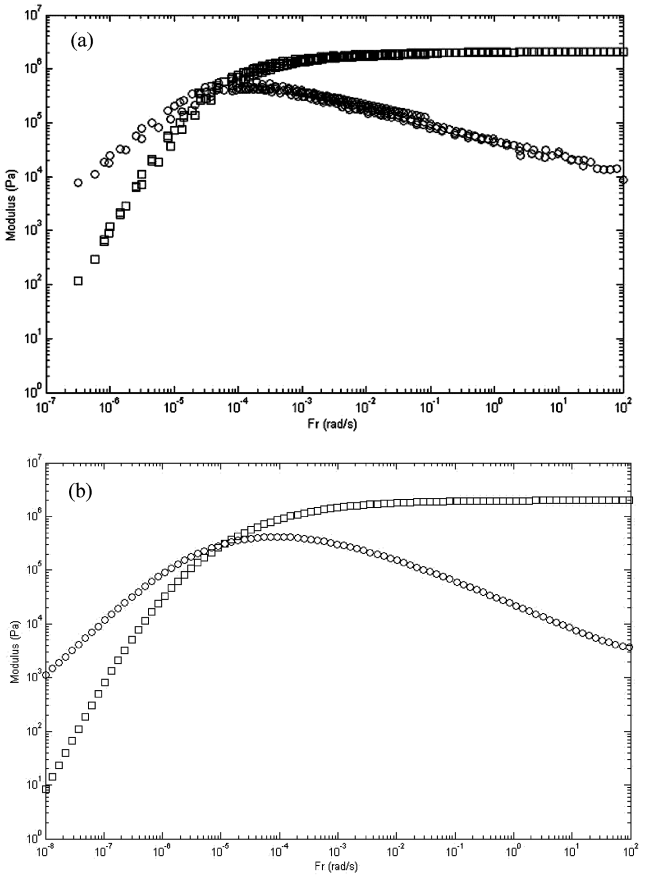


**Figure 11.** (a) Master curves for the reference sample, batch no. 5, having molar mass of $9.1 \times 10^6$ g/mol. $G'$ and $G''$ are depicted by open squares and circles, respectively. The storage and loss modulus over the wide frequency region are obtained by shifting the modulus data horizontally for a range of polymers. (b) Theoretically determined dynamic data from molar mass data. Crossover point matches well from both methods that it occurs at frequency around $1 \times 10^{-5}$ to $2 \times 10^{-5}$ rad/s.

high-molar-mass polymers can be predicted using this shift factor.

For plotting of the master curve, it is assumed that the synthesized UHMWPE samples possess similar polydispersities as the low-molar-mass polyethylenes presented in Figure 10. Considering GPC data and frequency sweep results (Figure 5) and taking similar synthesis conditions (controlled polymerization) into consideration, this assumption seems reasonable. Therefore, it is expected that the chain dynamics in UHMWPE having a number-average molar mass $>10^6$ g/mol should be similar to the linear monodisperse polyethylene shown in Figure 10, except that the terminal region will be shifted to much lower frequencies. The result of time-MW superposition for highest molar mass sample, batch no. 5, having molar mass of $9.1 \times 10^6$ g/mol, is illustrated in Figure 11a. The terminal region representing the overall chain dynamics is extended to very low frequency, $10^{-7}$ rad/s.

Figure 11b shows extended dynamic data obtained from the model (eq 2). From Figure 11, it is apparent that the theoretical data (Figure 11b) match well with the experimental results described in Figure 11a. Interestingly, the value of the crossover point and zero shear viscosity obtained experimentally ($2.1 \times 10^{-5}$ rad/s, $9.5 \times 10^{10}$ Pa·s) and theoretically ($1.1 \times 10^{-5}$ rad/s, $1.3 \times 10^{11}$ Pa·s) are quite similar. Therefore, the determined molar mass and molar mass distribution, as depicted by rheometry in Table 2 for the sample batch no. 5, is a good estimate. We will like to stress that the polymers that have been investigated in this publication have a PDI that may change from 1.1. to 2.3, but the number-average molar mass stays $>1\,000\,000$ g/mol. Therefore, relaxation times of even the lowest molar mass chains in the samples having PDI 2.3 are far from the highest sharp molar mass distributed polymer having the PDI 1.1. The high number-average molar mass combined with the linear nature of the chain provides the possibility of using the described method in this article for the determination of molar mass and molar mass distribution.

## Conclusions

It is shown that melt rheology can provide information on the molar mass and molar mass distribution of ultra-high-molar-mass polyethylene samples synthesized using the living single-site catalyst. By tuning polymerization time and temperature and choosing the appropriate solvent and catalyst, UHMWPE can be obtained with extremely high molar masses of up to $10^7$ g/mol with extremely high number-average molar mass. Molar mass and PDI of the thus-synthesized polymer have been measured by means of melt rheometry and size exclusion chromatography techniques. Our preferred method is melt rheometry based on a modulus model. Considering the good match (within experimental limitations) between the experimental and theoretical data, it is concluded that the applied rheological techniques to determine the high molar mass work reasonably good for the linear polymer with relatively high number-average molar mass. These findings are of relevance in determining very high molar masses that cannot be obtained conclusively with the existing chromatography techniques. An important factor to determine such high molar masses via melt rheological methods is the availability of the onset of the terminal region data in the modulus-frequency diagram. The onset of the terminal region data is obtained by converting the static data into the dynamic data. The static data is obtained from the stress-relaxation experiments, where the creep experiments due to high melt viscosity impose restrictions.

**Acknowledgment.** We thank professor Münstedt for providing the desired GPC facilities in his laboratories. Saeid Talebi was awarded a scholarship from the Sahand University of Technology funded by the Ministry of Science of I.R. Iran. He thanks both organizations for the financial support. We also extend thanks to Professor Spiess and his group from MPIP-Mainz for the ongoing research collaboration on solid-state NMR; some of these studies are mentioned in this publication.

**Supporting Information Available:** Reproducibility of GPC measurements for different molar masses. This material is available free of charge via the Internet at http://pubs.acs.org.

## References and Notes

(1) Soga, K.; Shiono, K. *Prog. Polym. Sci.* **1997**, *22*, 1503.
(2) (a) Domskia, G. J.; Rosea, J. M.; Coates, G. W.; Boligb, A. D.; Brookhartb, M. *Prog. Polym. Sci.* **2007**, *32*, 30. (b) Coates, G. W.; Hustad, P. D.; Reinartz, S. *Angew. Chem., Int. Ed.* **2002**, *40*, 2236.
(3) (a) Matsui, S.; Tohi, Y.; Mitani, M.; Saito, J.; Makio, H.; Tanaka, H.; Nitabaru, M.; Nakano, T.; Fujita, T. *Chem. Lett.* **1999**, 1065. (b) Matsui, S.; Mitani, M.; Saito, J.; Tohi, Y.; Makio, H.; Tanaka, H.; Fujita, T. *Chem. Lett.* **1999**, 1263. (c) Matsui, S.; Mitani, M.; Saito, J.; Matsukawa, N.; Tanaka, H.; Nakano, T.; Fujita, T. *Chem. Lett.* **2000**, 554. (d) Fujita, T.; Tohi, Y.; Mitani, M.; Matsui, S.; Saito, J.; Nitabaru, M.; Sugi, K.; Makio, H.; Tsutsui, T. Eur. Pat. Appl. 874005. (e) Nakano, T.; Tanaka, H.; Kashiwa, N.; Fujita, T. PCT Int. Appl. WO2001055231.
(4) (a) Tian, J.; Coates, G. W. *Angew. Chem.* **2000**, *112*, 3772. (b) *Angew. Chem., Int. Ed.*, **2000**, *39*, 3626.
(5) (a) Mitani, M.; Mohri, J.-I.; Yoshida, Y.; Saito, J.; Ishii, S.; Tsuru, K.; Matsui, S.; Furuyama, R.; Nakano, T.; Tanaka, H.;

Kojoh, S.-I.; Matsugi, T.; Kashiwa, N.; Fujita, T. *J. Am. Chem. Soc.* **2002**, *124*, 7888. (b) Mitani, M.; Nakano, T.; Fujita, T. *Chem.—Eur. J.* **2003**, *9*, 2396.
(6) Saito, J.; Mitani, M.; Mohri, J.-I.; Yoshida, Y.; Matsui, S.; Ishii, S.-I.; Kojoh, S.-I.; Kashiwa, N.; Fujita, T. *Angew. Chem.* **2001**, *113*, 3002.
(7) Sharma K. *Easily Processable UHMWPE with Narrow Molecular Weight Distribution*. Ph.D. Thesis, Eindhoven University of Technology, **2005**.
(8) Rastogi, S.; Lippits, D.; Peters, G. W. M.; Graf, R.; Yao, Y.-F.; Spies, H. W. *Nat. Mater.* **2005**, *4*, 635.
(9) Lippits, D. R.; Rastogi, S.; Talebi, S.; Bailly, C. *Macromolecules* **2006**, *39*, 8882.
(10) Zimm, B. H. *J. Chem. Phys.* **1948**, *16*, 1099.
(11) From the private report kindly provided by Dr. J. Kaschta, Group of Prof. H. Münstedt in the Institute of Polymer Materials at the Erlangen University.
(12) (a) Ivanchev, S. S.; Badaev, V. K.; Ivancheva, N. I.; Khaikin, S. Ya. *Dokl. Phy. Chem.* **2004**, *394*, 46. (b) Ivanchev, S. S.; Trunov, V. A.; Rybakov, V. B.; Al'bov, D. V.; Rogozin, D. G. *Dokl. Phys. Chem.* **2005**, *404*, 165.
(13) Atiqullah, M.; Hammawa, H.; Hamid, H. *Eur. Polym. J.* **1998**, *34*, 1511.
(14) Huang, J.; Rempel, G. L. *Prog. Polym. Sci.* **1995**, *20*, 459.
(15) Kaminsky, W.; Kulper, K.; Niedoba, S. *Makromol. Chem., Macromol. Symp.* **1986**, *3*, 377.
(16) Chein, J. C. W.; Sugimoto, R. *J. Poly. Sci., Polym. Chem. Ed.* **1990**, *28*, 15.
(17) Saito, J.; Mitani, M.; Matsui, S.; Tohi, Y.; Makio, H.; Nakano, T.; Tanaka, H.; Kashiwa, N.; Fujita, T. *Macromol. Chem. Phys.* **2002**, *203*, 59.
(18) (a) Kaminsky, W.; Steiger, R. *Polyhedron* **1988**, *7*, 2375. (b) Corradini, P.; Guerra, G. *Prog. Polym. Sci.* **1991**, *16*, 239.
(19) Dos Santos, J. H. Z.; Grecco, P. P.; Stedile, F. C.; Chornik, B. *J. Mater. Online* **2006**, *2*, 1.
(20) (a) Kaminsky, W. *J. Mol. Catal.* **1992**, *74*, 109. (b) *Macromol. Symp.* **1995**, *97*, 79. (c) *Macromol. Chem. Phys.* **1996**, *197*, 3907.
(21) Chein, J. C. W.; Wang, B.-P. *J. Polym. Sci., Part A: Polym. Chem.* **1990**, *28*, 15.
(22) (a) Rieger, B.; Janiak, C. *Angew. Makromol. Chem.* **1994**, *215*, 35. (b) Estrada, J. M. V.; Hamielec, A. E. *Polymer* **1994**, *35*, 808. (c) D'Agnillo, L.; Soares, J. B. P.; Penlidis, A. *Macromol. Chem. Phys.* **1998**, *199*, 955.
(23) Pollard, M.; Klimke, K.; Graf, R.; Spiess, H. W.; Wilhelm, M.; Piel, S. C.; Kaminsky, W. *Macromolecules* **2004**, *37*, 813.
(24) Bersted, B. H. *J. Appl. Polym. Sci.* **1975**, *19*, 2167.
(25) Bersted, B. H.; Slee, J. D. *J. Appl. Polym. Sci.* **1977**, *21*, 2631.
(26) Colby, R. H.; Fetters, L. J.; Graessley, W. W. *Macromolecules* **1987**, *20*, 2226.
(27) Malkin, A. Ya.; Teishev, A. E. *Polym. Eng. Sci.* **1991**, *31*, 1590.
(28) Tuminello, W. H. *Polym. Eng. Sci.* **1991**, *31*, 1496.
(29) Nichetti, D.; Manas-Zloczower, I. *J. Rheol.* **1998**, *42*, 951.
(30) Ferry J. D., *Viscoelastic Properties of Polymers*; Wiley: New York, 1980.
(31) Wu, S. *Polym. Eng. Sci.* **1985**, *25*, 122.
(32) de Gennes, P. G. *Scaling Concepts in Polymer Physics*; Cornell University Press: Ithaca, NY, 1979.
(33) Doi, M.; Edwards, S. F. *The Theory of Polymer Dynamics*; Clarendon: Oxford, U.K., 1986.
(34) Rubinstein, M.; Colby, R. H. *J. Chem. Phys.* **1988**, *89*, 5291.
(35) (a) des Cloizeaux, J. *Europhys. Lett.* **1998**, *5*, 417. (b) des Cloizeaux, J. *J. Phys. I* **1993**, *3*, 61.
(36) Tsenoglou, C. *J. Polym. Sci., Part B: Polym. Phys.* **1988**, *26*, 2329.
(37) Marrucci, G. *J. Polym. Sci.* **1985**, *23*, 159.
(38) Rubinstein, M.; Helfand, E.; Pearson, D. S. *Macromolecules* **1987**, *20*, 822.
(39) van Ruymbeke, E.; Keunings, R.; Stéphenne, V.; Hagenaars, A.; Bailly, C. *Macromolecules* **2002**, *35*, 2689.
(40) van Ruymbeke, E.; Keunings, R.; Bailly, C. *J. Non-Newtonian Fluid Mech.* **2002**, *105*, 153.
(41) Mead, D. W. *J. Rheol.* **1994**, *38*, 1739; **1994**, *38*, 1797.
(42) Rheometric Scientific, Inc., Product Brirf.
(43) Carrot, C.; Guillet, J. *J. Rheol.* **1997**, *41*, 1203.
(44) Plazek, D. J.; Raghupathi, N.; Orbon, S. J. *J. Rheol.* **1979**, *23*, 477.
(45) Schwarzl, F. R. *Rheol. Acta* **1975**, *14*, 581.
(46) Kraft, M.; Meissner, J.; Kaschta, J. *Macromolecules* **1999**, *32*, 751.
(47) Stadler, F. J.; Piel, C.; Klimke, K.; Kaschta, J.; Parkinson, M.; Wilhelm, M.; Kaminsky, W.; Münstedt, H. *Macromolecules* **2006**, *39*, 1474.
(48) Stadler, F. J.; Piel, C.; Kaminsky, W.; Münstedt, H. *Macromol. Symp.* **2006**, *236*, 209.